A 3.5-GHz Band 140-W-Class Wideband Feed-Forward Power Amplifier for Mobile Base Stations

Yasunori Suzuki, Junya Ohkawara, and Shoichi Narahashi

Research Laboratories, NTT DOCOMO, INC.
3-6 Hikari-no-oka, Yokosuka, Kanagawa 239-8536 Japan
suzukiyasu@nttdocomo.co.jp
ookawaraj@nttdocomo.co.jp
narahashi@nttdocomo.co.jp

Abstract

This paper analyzes the characteristics when compensating for wideband intermodulation distortion (IMD) components of a fabricated 3.5-GHz band 140-W class feed-forward power amplifier (FFPA) for mobile base stations. The fabricated FFPA achieves the bandwidths of 160 MHz and 120 MHz when compensating for the IMD components for LTE signals with the bandwidths of 5 MHz and 20 MHz, respectively, when the output power is 40 dBm and the adjacent channel leakage power ratio is -45 dBc. Experimental and analysis results show that the FFPA compensates for the wideband IMD components when the IMD component compensation level is reduced. This paper shows that the FFPA is a worthwhile linearizer that compensates for 3.5-GHz band wideband IMD components.

1. Introduction

Mobile communication systems continuously evolve to offer novel mobile communication services toward international mobile telecommunications (IMT)-Advanced as specified by the International Telecommunication Union - Radiocommunication Sector. IMT-Advanced specifies that the data rate should be approximately 100 Mbps under high mobility conditions and 1 Gbps under low mobility or stationary conditions [1, 2]. The third generation partnership project has been investigating the long term evolution (LTE)-Advanced as IMT-Advanced [3]. The World Radiocommunication Conference 2007 adopted new primary allocations for mobile communication services and/or new identifications for the IMT-2000 and IMT-Advanced systems in a number of bands including 3.4 – 3.6 GHz [4, 5].

Base station power amplifiers will be required to provide wider bandwidth operation in the 3.5-GHz band. This indicates that the linearizer of the base station power amplifier will also be required to have the capability to compensate for wideband intermodulation distortion (IMD) components. There are two major types of linearizers for base stations: one is the "digital predistortion linearizer (DPDL)" and the other is a "feed-forward" type. The DPDL is used in IMT-2000 base stations [6]. Application of the DPDL may be effective as a wideband IMD component compensation technique such as over a 100-MHz bandwidth in the future. In this case, the digital signal processing unit of the DPDL requires an operational bandwidth of several hundred megahertz taking the oversampling rate and the third-order and fifth-order IMD components into account. On the other hand, it is known that the feed-forward power amplifier (FFPA) can compensate for wideband IMD components in principle [7-9]. Previously, we presented an experimental investigation on the characteristics of wideband IMD compensation for a 3.5-GHz band FFPA employing an LTE test signal with a 5-MHz bandwidth [10]. However, there is still insufficient discussion regarding the bandwidth when compensating for IMD components using other test signals. This paper analyzes the characteristics when compensating for wideband IMD components for a fabricated 3.5-GHz band 140-W class FFPA employing LTE test signals with bandwidths of 5 MHz and 20 MHz. This paper also discusses the characteristics when compensating for wideband IMD components based on experimental and numerical results.

2. Analysis

The FFPA has two loops: One is the signal cancellation loop and the other is the distortion cancellation loop. Fig. 1 shows a basic configuration corresponding to the signal cancellation loop and the distortion cancellation loop. The basic configuration has a delay line and a vector regulator that adjusts the amplitude and phase of the input signal. From the standpoint of frequency characteristic analysis, the vector regulator is assumed to have flat frequency characteristics and the delay time of zero. The output signal, y, of the basic configuration can be expressed as

$$y = \left(\exp\left(-j2\pi f\tau\right) - a\exp\left(j\theta\right)\right)x . \quad (1)$$

Here x is the input signal of the basic configuration, and a and θ are the amplitude and phase errors of the vector regulator, respectively. Terms f and τ are the frequency offset from the center frequency of x and the delay mismatch of

978-1-4244-6051-9/11/$26.00 ©2011 IEEE

the delay line at the center frequency of x, respectively. The frequency offset corresponds to the bandwidth. The signal suppression level, $|y/x|^2$, can be expressed as

$$\left|y/x\right|^2 = 1 + a^2 - 2a\cos\left(\theta + 2\pi f\tau\right) . \quad (2)$$

Fig. 2 shows the numerical calculation results of (2). The signal suppression ratio and the frequency offset are indicated on the vertical and horizontal axes, respectively. The phase error offsets the frequency at the minimum signal suppression ratio from the frequency at the phase error of zero. From Fig. 2, the phase error of 10 deg. has the frequency offset of 3 MHz. On the other hand, the amplitude error reduces the signal suppression ratio. The amplitude error of 0.45 dB becomes the minimum signal suppression ratio of -20 dB. Fig. 3 shows the numerical calculation results of (2). The relative bandwidth and the signal suppression level are indicated on the vertical and horizontal axes, respectively. The relative bandwidth corresponds to $f\ \tau$*100. It is the same as the ratio of the signal bandwidth to the center frequency. The relationship between the signal suppression ratio and the relative bandwidth does not depend on the phase error because the phase error only causes the frequency offset from the minimum signal suppression ratio shown in Fig. 2. When the amplitude error and the phase error are zero, the signal suppression level depends on the relative bandwidth. For example, the signal suppression level is 30 dB at the relative bandwidth of 1% (the bandwidth of 35 MHz at the center frequency of 3.5 GHz). Furthermore, the signal suppression level is saturated more than that at the relative bandwidth of about 4% when the amplitude error is from 0 dB to 1.0 dB. Fig. 3 shows that the FFPA can suppress the wideband IMD components, but the signal suppression level is reduced.

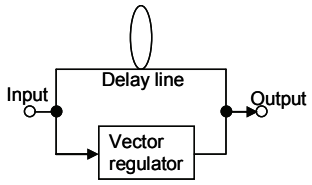

Fig. 1. Basic configuration of the signal cancellation loop and the distortion cancellation loop.

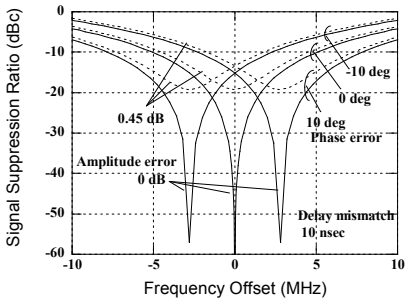

Fig. 2. Numerical calculation results showing relationship between the signal suppression level and frequency offset.

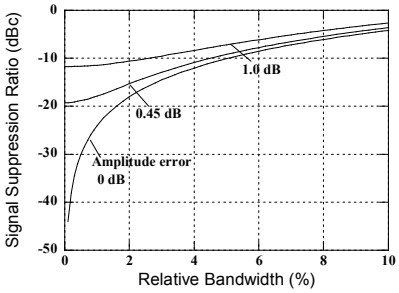

Fig. 3 Numerical calculation results showing relationship between the signal suppression level and the relative bandwidth.

3. Experiment

3.1 Fabricated FFPA

Figs. 4 and 5 show the configuration and a photograph of the fabricated FFPA that employs self-adjusting circuits for the signal and distortion cancellation loops. The fabricated FFPA is designed with the center frequency of 3.5 GHz. The main amplifier is a harmonic reaction amplifier (HRA) [11] that has a 3.5-GHz signal rejection filter, a second harmonic 7.0-GHz rejection filter, and a second harmonic path. The main amplifier uses two 70-W class GaN HEMTs in class-AB biasing. The saturation output power is approximately 51.5 dBm using a pulse test signal. The error amplifier uses a 70-W class GaN HEMT with class-A biasing. The self-adjusting circuits consist of pilot signal generators, pilot signal detectors, and a controller [9]. The controller adjusts the vector regulator to achieve the minimum level for the detected pilot signal.

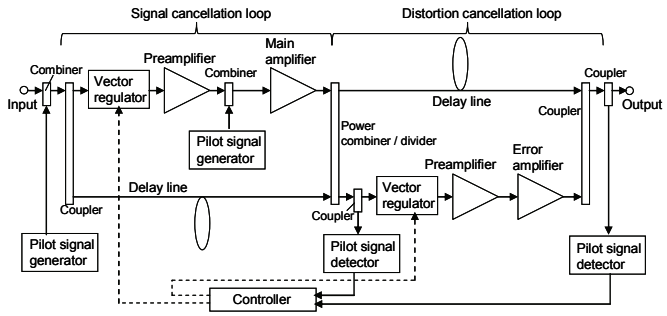

Fig. 4. Fabricated FFPA configuration.

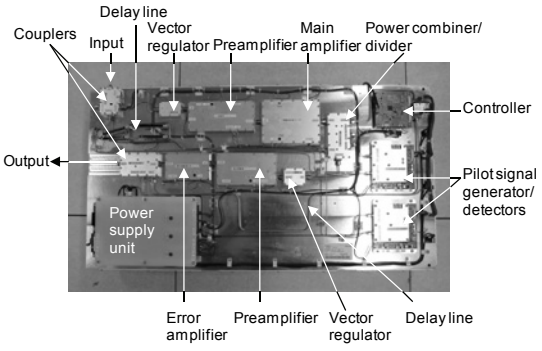

Fig. 5. Photograph of fabricated FFPA.

3.2 Test Signals

The test signals use LTE signals employing evolved universal terrestrial radio access test mode 1.1 [12]. The channel bandwidths of the test signals are 5 MHz and 20 MHz. The modulation scheme is QSPK. The number of resource blocks for the test signals with the bandwidths of 5 MHz and 20 MHz are 25 and 100 blocks, respectively. The complementary cumulative distribution functions of the test signals are almost the same as that for Gaussian noise. The peak-to-average power ratio (PAPR) of the test signals with the bandwidths of 5 MHz and 20 MHz are 9.4 dB and 11.1 dB, respectively. The vector signal generator outputs the test signals. The adjacent channel leakage power ratio (ACLR) is monitored by the spectrum analyzer. The ACLR of the test signal with the 5-MHz bandwidth is calculated from the ratio of the adjacent channel bandwidth of 4.515 MHz with a 5-MHz offset and the transmission bandwidth of 4.515 MHz [13]. The ACLR of the test signal with the 20-MHz bandwidth is calculated from the ratio of the adjacent channel bandwidth of 18.015 MHz with a 20-MHz offset and the transmission bandwidth of 18.015 MHz [13].

3.3 Results

Fig. 6 shows the output power performance of the fabricated FFPA at the measurement frequency of 3.5 GHz. The input power and the output power are represented on the vertical and horizontal axes, respectively. The power meters measured the input power and the output power, respectively. The controller is used to control the vector regulators. In this experiment, the vector regulators are set with the same amplitude and phase parameters as when employing the test signals with the bandwidths of 5 MHz and 20 MHz. The fabricated FFPA achieves the gain of 37 dB when using the test signals with the bandwidths of 5 MHz and 20 MHz.

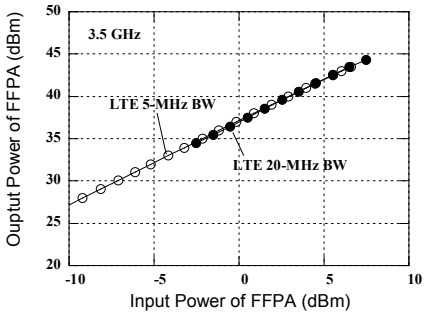

Fig. 6. Output power performance of fabricated FFPA with LTE test signals.

Fig. 7 shows the ACLR performance of the fabricated FFPA and the fabricated main amplifier at the measurement frequency of 3.5 GHz. The ACLR and the output power are indicated on the vertical and horizontal axes, respectively. We measured the lower ACLR and the upper ACLR simultaneously. The controller is used to control the vector regulators. In this experiment, the vector regulators are set with the same amplitude and phase parameters as when employing the test signals with the bandwidths of 5 MHz and 20 MHz. Fig. 6 shows the worst ACLR data of the measured ACLRs. The fabricated FFPA achieves the ACLR of -50 dBc with the test signal with the 20-MHz bandwidth and that of -58 dBc with the test signal with the 5-MHz bandwidth at the output power of 40 dBm. On the other hand, the fabricated main amplifier attains the ACLR of -32 dBc with the test signal with the 20-MHz bandwidth and that of -33 dBc for the test signal with the 5-MHz bandwidth at the output power of 40 dBm. The ACLRs of the test signal with the 20-MHz bandwidth are less than those for the test signal with the 5-MHz bandwidth. This is because the relative bandwidth of the test signal with the 20-MHz bandwidth is four times that for the test signal with the 5-MHz bandwidth, when the amplitude error and the phase error maintain the same levels.

Fig. 8 shows the frequency characteristics of the ACLR in the fabricated FFPA with the test signals with the bandwidths of 5 MHz and 20 MHz. The ACLR and the frequency are represented on the vertical and horizontal axes, respectively. The output power is 40 dBm because the output back-off level is the same as the PAPR of the test signal with the 20-MHz bandwidth. The vector regulators are manually set to minimize the ACLRs monitored by the spectrum analyzer at 3.5 GHz. The ACLRs at each frequency are measured when the center frequencies of the test signal are changed. The frequency span is set to 20 MHz. The ACLR compensation bandwidth of the fabricated FFPA at the ACLR of -45 dBc is 160 MHz with the test signal with the 5-MHz bandwidth and 120 MHz in the test signal with the 20-MHz bandwidth. In this case, the minimum ACLR compensation level with the test signal with the 20-MHz bandwidth deteriorates by 8 dB from that with the test signal with the 5-MHz bandwidth. The experimental results show that the fabricated FFPA compensates for the distortion in the wideband IMD components. The frequency characteristics of the ACLR with the test signal with the 20-MHz bandwidth become the same those for the ACLR level

of the test signal with the 5-MHz bandwidth when the frequency offset is more than 50 MHz. The FFPA compensates for the wideband IMD components and reduces the IMD component compensation level shown in Fig. 3.

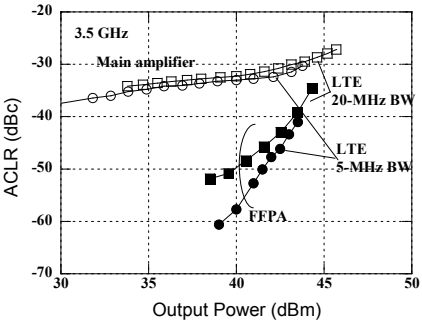

Fig. 7. ACLR performance with LTE test signals.

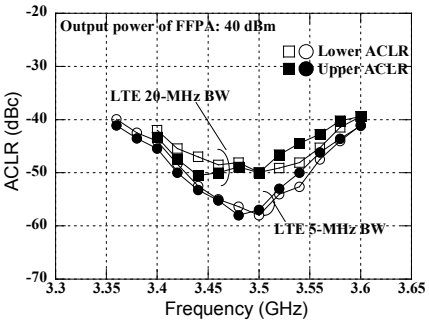

Fig. 8. Frequency characteristics of ACLR.

4. Conclusion

This paper presented the compensation characteristics for the wideband IMD components of the FFPA. The analytical results indicated that the FFPA compensates for the wideband IMD components when the compensation level for the IMD components is reduced. The fabricated FFPA achieved the bandwidths of 160 MHz and 120 MHz when compensating for the IMD components for LTE signals with the bandwidths of 5 MHz and 20 MHz, respectively, when the output power is 40 dBm and the ACLR is -45 dBc. The minimum ACLR level in the LTE test signal with the 20-MHz bandwidth was deteriorated by 8 dB from that for the LTE test signal with the 5-MHz bandwidth. The FFPA provides the wideband IMD components compensation performance in the 3.5-GHz band. From the experimental and numerical results, the feed-forward technique is a worthwhile wideband linearization technique and is an alternative approach against DPDL techniques. There still remain technical issues such as reducing the power consumption when compensating for the wideband IMD components.

5. References

1. Recommendation ITU-R M.1645, "*Framework and Overall Objectives of the Future Development of IMT-2000 and Systems Beyond IMT-2000*," June 2003.
2. Y. K. Kim, and R. Prasad, *4G Roadmap and Emerging Communication Technologies*, Artech House, 2006.
3. S. Parkvall, E. Dahlman, A. Furuskar, Y. Jading, M. Olsson, S. Wanstedt, K. Zangi, "LTE-Advanced – Evolving LTE Towards IMT-Advanced," *Proc. of IEEE 68th Vehicular Technology Conference*, Sept. 2008, pp. 21-24.
4. A. Hashimoto, H. Yoshino, and H. Atarashi, "Roadmap of IMT-Advanced Development," *IEEE Microwave Magazine*, Aug. 2008, pp. 80-88.
5. H. Takagi, and B. H. Walke, *Spectrum Requirement Planning in Wireless Communications --- Model and Methodology for IMT-Advanced*, John Wiley & Sons, 2008.
6. Y. Oishi, N. Tozawa, and H. Suzuki, "Highly Efficient Power Amplifier for IMT-2000 BTS Equipment," *FUJITSU Sci. Tech. J.*, **38**, 2, Dec. 2002, pp. 201-208.
7. H. Seidel, "A Microwave Feed-Forward Experiment," *Bell System Tech. Jour.*, **50**, 9, 1971, pp. 2789-2916.
8. N. Pothecary, *Feedforward Linear Power Amplifier,* Artech House, 1999.
9. S. Narahashi and T. Nojma, "Extremely Low-Distortion Multi-carrier Amplifier --- Self-adjusting Feed-Forward (SAFF) Amplifier ---," *Proc. IEEE ICC'91*, 1991, pp. 46.5.1-46.5.6.
10. Y. Suzuki, J. Ohkawara, and S. Narahashi, "Experimental Investigation on Wideband Intermodulation Distortion Compensation Characteristics of 3.5-GHz band 140-W Class Feed-Forward Power Amplifier Employing GaN HEMTs," *Proc, of the 2010 Asia-Pacific Microwave Conference*, **WE1A-1**, Dec. 2010.
11. S. Nishiki and T. Nojima, "Harmonic Reaction Amplifier --- A Novel High Efficiency and High-Power Microwave Amplifier ----," *Proc. IEEE MTT-S Int. Microwave Symp. Digest*, **DD-5**, 1987, pp. 963-966.
12. 3GPP TS35.141, "Evolved Universal Terrestrial Radio Access (E-UTRA): Base Station (BS) Conformance Testing," 2010.
13. 3GPP TS36.104, "Evolved Universal Terrestrial Radio Access (E-UTRA): Base Station (BS) Radio Transmission and Reception," 2008.